

Suzaku Reveals He-burning Products in the X-ray Emitting Planetary Nebula BD +30° 3639

M. Murashima¹, M. Kokubun¹, K. Makishima^{1,2}, J. Kotoku³, H. Murakami⁴,
K. Matsushita⁵, K. Hayashida⁶, K. Arnaud⁷, K. Hamaguchi⁷, and H. Matsumoto⁸

1: Department of Physics, University of Tokyo, 7-3-1 Hongo, Bunkyo-ku, Tokyo 113-0011, Japan

2: The Institute of Physical and Chemical Research, 2-1 Hirosawa, Wako, Saitama 351-0198, Japan

3: Department of Physics, Tokyo Institute of Technology, O-okayama, Meguro-ku, Tokyo 152-8551, Japan

4: PLAIN Center, ISAS/JAXA, 3-1-1 Yoshinodai, Sagami-hara, Kanagawa 229-8510, Japan

5: Department of Physics, Tokyo University of Science, Kagurazaka, Shinjuku-ku, Tokyo 162-8601, Japan

6: Department of Space and Earth Science, Osaka University, Toyonaka, Osaka 560-0043, Japan

7: Exploration of the Universe Division, Code 660, NASA/GSFC, Greenbelt, MD 20771, USA

8: Department of Physics, Kyoto University, Kitashirakawa, Sakyo-ku, Kyoto 606-8502, Japan

ABSTRACT

BD +30° 3639, the brightest planetary nebula at X-ray energies, was observed with *Suzaku*, an X-ray observatory launched on 2005 July 10. Using the X-ray Imaging Spectrometer, the K-lines from C VI, O VII, and O VIII were resolved for the first time, and C/O, N/O, and Ne/O abundance ratios determined. The C/O abundance ratio exceeds the solar value by nearly two orders of magnitude, and that of Ne/O by at least a factor of 5. These results indicate that the X-rays are emitted mainly by helium shell-burning products.

Subject headings: planetary nebulae: general — planetary nebulae: individual(BD +30° 3639), X-ray

1. Introduction

Intermediate-mass stars, with initial masses $\lesssim 8 M_{\odot}$, are thought to contribute significantly to the synthesis of C, N, O, and Ne through the CNO cycle and He burning. These nuclear fusion products are ejected through mass loss as the stars evolve from their AGB phase into planetary nebulae (PNe). Hence, a PN can be regarded as a messenger bearing information on the nucleosynthesis within these stars. However, the optically-visible material in PNe represents matter accumulated over the PN lifetime, making it difficult to extract information on, for instance, pure He-burning products just by observing the PNe shells.

Soft X-rays, detected from several PNe, are thought to originate in hot plasmas produced by shocks in fast stellar winds (Kwok 1982; Volk & Kwok 1985). These fast winds develop during the later evolutionary stages of the central star, so the X-rays are thought to be emitted by the star's late-

phase products. X-ray spectroscopy of PNe will thus allow us to diagnose products of a particular nucleosynthesis phase inside intermediate-mass stars. However, it has been difficult to resolve K-lines from C, N, and O, the major CNO and He-burning products, because the line energies are too low for X-ray CCDs and the PNe are too faint for high-resolution spectroscopy using gratings.

The 5th Japanese X-ray satellite *Suzaku* (*Astro-E2*; Mitsuda et al. 2004) was developed by a Japan-US collaboration as a successor to *ASCA*, and was launched successfully on 2005 July 10. Its X-ray Imaging Spectrometer (XIS) comprises four CCD cameras, XIS-0 through XIS-3 (Hayashida et al. 2004). Three of the cameras use front-illuminated (FI) CCD chips while XIS-1 utilizes the back-illuminated (BI) technology. Compared to similar instruments on preceding X-ray missions, both the BI and FI chips have better responses to X-rays with energies below ~ 1 keV.

We observed the PN, BD +30° 3639, with *Suzaku* in order to resolve the anticipated carbon and oxygen emission lines. Since its detection using *ROSAT* (Kreysing et al. 1992), this object has been known as the X-ray brightest PN, emitting spatially-extended soft X-rays from inside its $\sim 4''$ diameter optical shell (Kastner et al. 2000). The X-ray emitting plasma is thought to have highly non-solar abundance ratios, as shown by the strong Ne-K line first detected using *ASCA* (Arnaud et al. 1996), and a broad sub-keV spectral hump, presumably a blend of C, N, and O lines, subsequently detected with *Chandra* (Kastner et al. 2000; Maness et al. 2003).

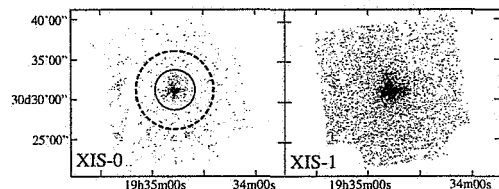


Fig. 1.— Images of BD +30° 3639 in 0.3–0.7 keV, taken with XIS-0 (FI-CCD; left) and XIS-1 (BI-CCD; right). Two circles specify data accumulation regions.

2. Observation

The present observation of BD +30° 3639 was performed for a net exposure of 34.4 ksec on 2005 September 20 (seq. no. 100025010), as part of the initial performance verification of *Suzaku*. Both the XIS and the Hard X-ray Detector (HXD; Kawaharada et al. (2004)) onboard were operated in their nominal modes. We do not use the HXD data since its non-imaging $34' \times 34'$ field of view also contains part of the large supernova remnant, G65.2+5.7, which overlaps with the target PN.

The target was clearly detected in all XIS cameras and is unresolved at the angular resolution of the *Suzaku* X-ray Telescopes; Figure 1 shows 0.3–0.7 keV images obtained with two of the cameras. We define the source region as a $2'.5$ radius circle centered on the source, and the background region as a surrounding annulus with an outer radius of $5'$. After background subtraction, net signal counts are 1116 ± 46 , 3039 ± 74 , 1174 ± 47 , and 1012 ± 44 from XIS-0, 1, 2, and 3, respectively.

Since the three FI cameras (XIS-0, 2, 3) are essentially identical, we co-add their data, and refer to them as “XIS-023” below.

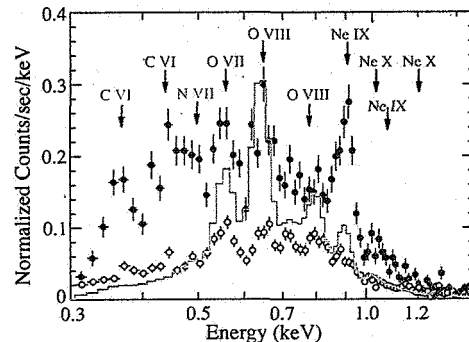


Fig. 2.— Spectra obtained with XIS-1 (BI). Red filled circles show the on-source (background inclusive) data, and black open circles the background. The prediction of an absorbed 1-solar abundance model with $kT = 0.2$ keV is sketched in green. Positions of major lines are indicated in blue.

3. Analysis and Results

As shown in Figure 2, the on-source XIS-1 spectrum clearly shows at 0.37 keV the K_{α} line from hydrogenic carbon (C VI). Its absence in the background spectrum ensures that the line is not due to contamination by G65.2+5.7. The spectra also show K_{α} lines from O VII, O VIII, and Ne IX.

At a temperature of $kT \sim 0.3$ keV (Arnaud et al. 1996; Maness et al. 2003), the C VI to O VII line emissivity ratio of a solar-ratio plasma is ~ 0.15 . This ratio will be reduced to ~ 0.03 (Murashima 2006) due to interstellar absorption, and the decrease in XIS-1 efficiency toward lower energies. Nevertheless, the XIS-1 spectrum yields comparable numbers of C VI and O VII line photons, suggesting a highly enhanced C/O ratio.

This early in the mission, the XIS calibration is still being fine-tuned. There are uncertainties in the energy gain, and also in the low-energy efficiency which has decreased since the start of observations. We solved the former by self-calibrating using the emission lines from BD +30° 3639 themselves. The latter effect is attributed to excess absorption due to the build-up of contaminant

in front of the XIS cameras. We estimated the chemical composition of the excess absorber using a *Suzaku* observation of the isolated neutron star RX J1856.6-3574 (Murashima 2006), which is known to exhibit a blackbody with a temperature of 63 eV (Burwitz et al. 2003). To determine the contaminant thickness for XIS-1 and (separately) XIS-023 we included in all analysis a simultaneous fit to the archival (ObsId 587) background-subtracted *Chandra* ACIS-S spectrum.

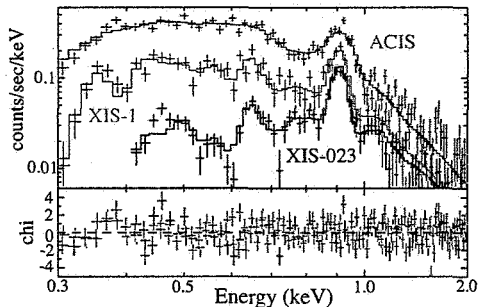


Fig. 3.— Background-subtracted XIS-1 (red), XIS-023 (black), and *Chandra* ACIS-S (blue) spectra of BD +30° 3639, fitted jointly by an absorbed vAPEC model. The XIS responses take into account the excess absorption.

We jointly fit the background-subtracted XIS-1, XIS-023, and *Chandra* ACIS-S spectra, using a single-temperature vAPEC model (Smith et al. 2001). The abundances (relative to solar; Anders & Gevesse (1989)) of C, N, O, Ne, and Fe, were left free; that of He fixed to solar; other heavy elements were neglected; kT and the hydrogen column density N_H were left free. As shown in Figure 3, the model gives a reasonable joint fit to the three spectra, with $\chi^2/\nu = 331/228$. We determined $kT = 0.19 \pm 0.01$ keV and $N_H = (2.1^{+0.4}_{-0.7}) \times 10^{21}$ cm $^{-2}$.

Figure 3 shows confidence contours for the C and O abundances, derived as described above. The absolute C and O abundances are poorly constrained, because the continua, due to hydrogen, (presumably non-solar abundance) helium, and the enhanced metals themselves, cannot be independently determined. Nevertheless, the individually resolved lines do successfully constrain the C/O ratio as $104 > C/O > 71$ solar at 90% confidence, with the best fit at 85. In the same way, we have obtained $5.5 > N/O > 0.9$ and $7.5 > Ne/O$

> 4.7 , with the best fits of 3.2 and 5.8, respectively, and $Fe/O < 0.1$, all in solar units.

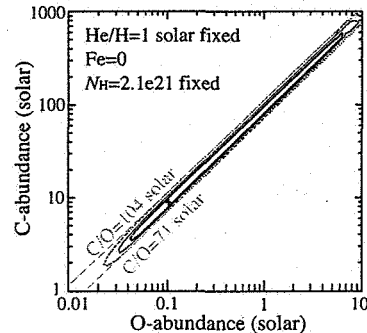


Fig. 4.— Confidence contours for the O and C abundances, derived from the single vAPEC fit of Figure 3. The 69% (black solid), 90% (red solid), and 99% (blue dotted) confidence contours are drawn. The other parameters are left free, except for those described in the figure.

Although we have so far assumed the He/H ratio to be solar, increasing it to 5, 10, or 20 solar does not affect the relative C/N/O/Ne abundances by more than 5%. Similarly, the results remain unchanged within $\sim 10\%$ when the thickness of the XIS excess absorber is varied by $\pm 20\%$ around the best estimates (equivalent to $N_H \sim 8 \times 10^{20}$ cm $^{-2}$), or the background spectra are derived from several other regions in the XIS field of view. If the absorption is fixed at the intervening interstellar column of 1×10^{21} cm $^{-2}$ (Murashima 2006) estimated from extinction (Cahn et al. 1992), the C/O ratio decreases by a factor of ~ 3 , but the (non-reduced) χ^2 increases by about 20.

To relax the assumption of isothermality, we refitted the three spectra jointly with a sum of two vAPEC components, which are constrained to share common abundances and the same N_H . We tentatively fixed the C/O ratio at various trial values, and let the two temperatures vary. Even with this extra degree of freedom, acceptable fits were reproduced only when the assumed C/O ratio is in the range 35–120 solar. Further, the C/O ratio stays above ~ 30 even when fitted with a model allowing non-equilibrium ionization conditions. Thus, the high C/O ratio is a robust result, confirming the previous suggestions (Arnaud et al. 1996; Kastner et al. 2000; Maness et al. 2003).

4. Discussion

At a distance of 1.3 kpc (Mellema 2004), the 0.2–2.0 keV luminosity of BD +30° 3639 is $\sim 1.4 \times 10^{33}$ ergs s⁻¹, in agreement with previous measurements. This is only $\sim 0.1\%$ of the kinetic luminosity supplied by the fast stellar wind (de Freitas Pacheco et al. 1993), $\sim 1.2 \times 10^{36}$ ergs s⁻¹. This, together with the X-ray emitting region just fitting inside the optical shell (Kastner et al. 2000), supports the interacting wind model (Kwok 1982; Volk & Kwok. 1985) as a baseline scenario to explain the X-ray emission from this PN.

Observations in the optical and neighboring wavelengths give the nebular abundance ratios of BD +30° 3639 as C/O ~ 3.7 , N/O ~ 1.8 , and Ne/O ~ 2.8 in solar units (Bernard-Salas et al. 2003). Compared with these, our X-ray results imply qualitatively similar, but much more extreme, abundance patterns. This is not surprising, since the X-ray emitting plasma is considered to represent a very limited radial zone of the stellar interior. In fact, assuming, based on the *Chandra* image, that the X-ray emitting plasma fills a sphere of radius 0.01 pc (1".6), its mass is estimated as $\sim 5 \times 10^{-4} M_{\odot}$ from the observed emission measure of 5.7×10^{55} cm⁻³. This can be supplied only in ~ 70 yr by the mass loss of $\sim 7 \times 10^{-6} M_{\odot}$ yr⁻¹ (de Freitas Pacheco et al. 1993).

Which part of the stellar interior provides the X-ray emitting plasma? The most outstanding feature is the extreme carbon enhancement, ~ 40 in the C/O *number* ratio; this is a typical value expected from competition between the triple- α and $^{12}\text{C}(\alpha, \gamma)^{16}\text{O}$ reactions during He shell-burning flashes (Suda et al. 2004), for an initial mass of $\sim 2 M_{\odot}$. Therefore, this suggests that the X-rays come primarily from He shell-burning products. The observed high Ne/O ratio, in contrast, requires a neon-producing path without ^{16}O . Presumably ^{14}N , from the CNO cycle, burnt as $^{14}\text{N}(\alpha, \gamma)^{18}\text{F}(\beta^+, \nu)^{18}\text{O}(\alpha, \gamma)^{22}\text{Ne}$ during the He shell flashes, producing ^{22}Ne which is indistinguishable in X-rays from the more abundant ^{20}Ne . Finally, the hint of enhanced N/O ratio suggests that some fraction of the nitrogen, produced in the CNO cycle and stored in the He layer, escaped without being caught up in the He shell burning.

From these considerations, we arrive at the following scenario for this PN. The hydrogen-rich en-

velope is likely to have already been expelled. The outer parts of the He layer, composed of radiative and convective zones, are currently being ejected in the form of fast stellar winds, carrying the abundant carbon and ^{22}Ne produced in He shell flashes, as well as unprocessed nitrogen. These ejecta are shock-heated to emit X-rays.

A more quantitative comparison with the optical spectra of the central stars of PNe (Leuenhagen & Hamann 1998) will provide a valuable calibration of the models of stellar evolution and nucleosynthesis. Such work may also allow us to estimate the initial progenitor mass, and to clarify when the fast stellar winds start blowing.

Authors thank Prof. M. Y. Fujimoto and Dr. T. Suda of Hokkaido University for elucidating discussion. MM expresses her deepest gratitude to *ASTRO-E/Astro-E2/Suzaku* project members.

Facilities: Suzaku (XIS).

REFERENCES

- Anders, E. & Grevesse, N. 1989, *Geochem. Cosmochem. Acta*, 53, 197
Arnaud, K., Borkowski, K. J., & Harrington, J. P. 1996, *ApJ*, 462, 75
Bernard-Salas, J., Pottasch, S. R., Wesselius, P. R., & Feibelman, W. A. 2003, *A&A*, 406, 165
Burwitz, V., Harbel, F., Neuhäuser, R., Predehl, P., Trümper, J., & Zavlin, V. E. 2003, *A&A*, 399, 1109
Cahn, J., Kaler, J., & Stanghellini, L. 1992, *A&AS*, 94, 399
de Freitas Pacheco, J. A., Costa, R. D. D., de Araujo, F. X., & Petrini, D. 1993, *MNRAS*, 260, 401
Hayashida, K., et al. 2004, *SPIE*, 5488, 73
Kawaharada, M. et al. 2004, *SPIE*, 5501, 286
Kastner, J. H., Soker, N., Vrtilik, S. D., & Dgani, R. 2000, *ApJ*, 545, 57
Kreysing, H. C., Diesch, C., Zweigle, J., Staubert, R., Grewing, M., & Hasinger, G. 1992, *A&A*, 264, 623
Kwok, S. 1982, *ApJ*, 258, 280
Leuenhagen, U., & Hamann, W.-R. 1998, *A&A*, 330, L265
Maness, H. L., Vrtilik, S. D., Kastner, J. H., & Soker, N. 2003, *ApJ*, 589, 439
Mellema, G. 2004, *A&A*, 416, 623
Mitsuda, K., Kunieda, H., Inoue, H., & Kelley, R. 2004, *SPIE*, 5488, 177
Murashima, M. 2006, PhD Thesis, the University of Tokyo
Smith, R. K., Brickhouse, N. S., Liedahl, D. A., & Raymond, J. C. 2001, *ApJ*, 556, L91
Suda, T., Aikawa, M., Machida, M. N., Fujimoto, M. Y., & Iben, I. J. 2004, *ApJ*, 611, 476
Volk, K., & Kwok, S. 1985, *A&A*, 153, 79

This 2-column preprint was prepared with the AAS L^AT_EX macros v5.2.